HHS Public Access

Author manuscript

Nat Chem Biol. Author manuscript; available in PMC 2014 March 01.

Published in final edited form as:

Nat Chem Biol. 2013 September ; 9(9): 535–539. doi:10.1038/nchembio.1298.

A Switch III Motif Relays Signaling between a B_{12} Enzyme and its G-protein Chaperone†

Michael Lofgren[1], **Dominique Padovani**[1,§], **Markos Koutmos**[2], and **Ruma Banerjee**[1,*]

[1]Department of Biological Chemistry, University of Michigan Medical School, Ann Arbor MI 48109-0600

[2]Department of Biochemistry & Molecular Biology, Uniformed Services University of the Health Sciences, Bethesda MD 28104

Abstract

Fidelity during cofactor assembly is essential for the proper functioning of metalloenzymes and is ensured by specific chaperones. MeaB, a G-protein chaperone for the coenzyme B_{12}-dependent radical enzyme, methylmalonyl-CoA mutase (MCM), utilizes the energy of GTP binding and/or hydrolysis to regulate cofactor loading into MCM, protect MCM from inactivation, and rescue MCM inactivated during turnover. Typically, G-proteins signal to client proteins using the conformationally mobile switch I and II loops. Crystallographic snapshots of MeaB reported herein reveal a novel switch III element, which exhibits substantial conformational plasticity. Using alanine-scanning mutagenesis, we demonstrate that the switch III motif is critical for bidirectional signal transmission of the GTPase activating protein activity of MCM and the chaperone functions of MeaB in the MeaB:MCM complex. Mutations in the switch III loop identified in patients corrupt this inter-protein communication and lead to methylmalonic aciduria, an inborn error of metabolism.

Metallochaperones control the specificity of metal insertion into active sites that harbor mononuclear sites, metalloclusters or organometallic cofactors[1–3]. The bacterial protein MeaB[4] and its human ortholog MMAA[5] are chaperones that regulate docking of coenzyme B_{12} (5′-deoxyadenosylcobalamin or AdoCbl) into the radical enzyme methylmalonyl-CoA mutase (MCM)[6,7]. MCM uses AdoCbl to catalyze the chemically challenging 1,2-rearrangement of (*R*)-methylmalonyl-CoA to succinyl-CoA[8]. Mutations in MCM or in MMAA result in methylmalonic aciduria, an inborn error of metabolism[5,9].

†This work was supported in part by a grant from the National Institutes of Health (DK45776).

*Corresponding Author: Tel: (734)-615-5238, FAX: (734)-763-7799, rbanerje@umich.edu.

§Present address. Laboratoire de Chimie et de Biochimie Pharmacologiques et Toxicologiques, CNRS UMR 8601, Université Paris Descartes, PRES Sorbonne Paris Cité, 45 rue des Saints Pères, 75006 Paris, France

Author Contributions

The contributions of each co-author to this study were as follows: ML (switch III mutants characterization, data analysis, writing), DP (preparation of MeaB for crystallization, edited paper), MK (crystallization studies, data analysis, writing), RB (data analysis, writing).

Competing financial interests

The authors declare no competing financial interests.

MeaB belongs to the G3E family of G-proteins that include other metallochaperones needed for nickel insertion into varied client proteins[10]. It forms a tight complex with MCM with affinities varying from 34–524 nM that is modulated by the ligand bound to each protein[11]. MeaB binds guanosine 5′-triphosphate (GTP) and guanosine 5′-diphosphate (GDP) with almost equal affinity and its low intrinsic GTPase activity is enhanced ~100-fold in the presence of MCM, which exhibits GTPase activating protein (GAP) activity[11]. MeaB in turn, orchestrates a complex series of actions powered by the energy of GTP binding or hydrolysis[6]. These functions include: (i) gating the transfer of AdoCbl from adenosyltransferase (ATR) to MCM while excluding the inactive precursor, cob(II)alamin, (ii) protecting MCM from oxidative inactivation during turnover, and (iii) reactivating via cofactor exchange, MCM that is inactivated during the catalytic cycle[6,12]. Chaperones with roles limited to reactivation have been described for methycobalamin-dependent methyltransferases and the AdoCbl-dependent subfamily of eliminases[13–18]. These chaperones either promote an adenosine 5′-triphosphate (ATP)-dependent exchange of inactive cobalamin for AdoCbl[16–19] or reduction of cob(II)alamin to cob(I)alamin during in situ repair of the cofactor on methyltransferases[13,20]. Insights into the mechanism by which complex bidirectional communication occurs between the active sites of MeaB and MCM have been lacking.

Classically, small G-proteins involved in signal transduction communicate via conformational changes in conserved switch I and II regions in response to nucleotide binding, exchange and/or hydrolysis[21]. MeaB is a homodimer and each subunit contains a central α/β G-domain core (Fig. 1a, light gray), a helical C-terminal extension (dark gray) contributing to the dimer interface and an N terminal extension[22] (medium gray). MeaB was previously crystallized in a nucleotide-free form (PDB ID: 2QM8; MeaB:2Pi) and in the presence of GDP (PDB ID: 2QM7; MeaB:2GDP)[22]. The location of the conformationally flexible switch I (residues 92-108) and II (residues 154-162) regions in MeaB used by G proteins for signal transmission via the canonical “spring-loaded” mechanism[23], had raised questions about how structural transitions accompanying nucleotide binding and GTP hydrolysis are communicated from MeaB to MCM[22]. The presence of phosphate in the crystallization conditions used to obtain the nucleotide-free structure had resulted in ordering of both P loops (residues 62-70) in the dimer. A comparison of MeaB structures has led us to identify switch III, a third mobile loop whose proximity to the GTPase active site and to the conserved switch II region, suggested the hypothesis that this structural element is utilized for nucleotide-responsive communication between the MeaB and the MCM active sites. Herein, we report the structures of apo- and 5′-guanylyl-β,γ-imidophosphate (GMPPNP)-bound MeaB and demonstrate using alanine scanning mutagenesis, the pleiotropic consequences of alterations to the switch III sequence. Our study identifies switch III as a critical structural element for bidirectional signaling between MeaB and MCM that is compromised by disease-causing mutations in the switch III loop identified in methylmalonic aciduria patients.

Results

Structure of Apo-MeaB and of MeaB•2GMPPNP

We report two new crystal structures of apo-MeaB in the absence of phosphate or sulfate and in the presence of the non-hydrolyzable GTP analogue, GMPPNP (Supplementary Results, Supplementary Table 1). The structure of apo-MeaB, unlike the earlier structures[22], comprises two dimers instead of a single dimer in the asymmetric unit (Supplementary Figure 1). Although the overall basic dimeric unit is very similar to the ones reported previously (Fig. 1a), there are discrete differences that are localized to the active site and the switch regions (Fig. 1a, Supplementary Figures 1–2). In one apo-MeaB dimer, the active sites are empty and the P-loops have conformations distinct from the reported MeaB structures. Thus, in the absence of nucleotides or phosphates, the P-loop rearranges and part of it forms an extra helical turn at the base of helix α4, increasing the number of turns from four to five (Supplementary Figure 1). This conformation is not conducive to substrate binding since the groove required for phosphate binding is not present. In the second dimer, there is a single GDP bound in one active site while the second active site is phosphate- and nucleotide-free with the P-loop in a conformation permissive for nucleotide binding (Supplementary Figure 1). We typically isolate “apo-MeaB” with 0.04 equivalents of bound GDP, which presumably represents nucleotide that remains associated with the protein during purification from cell extracts.

The MeaB•2GMPPNP structure exhibits an overall arrangement comparable to that of the other MeaB structures (Fig. 1a, Supplementary Figure 2). The overall conformation of the two monomers in each dimer is very similar. Although Mg^{2+} is required for the low intrinsic GTPase activity of MeaB (Supplementary Figure 3), it is not observed in any of the structures presumably because its binding site is not fully formed in the absence of MCM. The differences between the two monomers are primarily observed in the nucleotide-binding site and in the position of a loop (residues 177-188) referred to hereafter as Switch III (Fig 1a, right panel). There is clear electron density for GMPPNP in one of the monomers and residues K68, S69 and R108 contact the β- and γ-phosphates (Fig. 1b, chain A). In the second monomer (chain B), GMPPNP is bound in a different conformation in which the γ-phosphate, which exhibits only partial occupancy, is re-positioned and oriented away from the active site. It is more solvent exposed and interacts only with S69. In fact, the hydroxyl group of S69 in chain B is rotated by almost 180° and reoriented to interact directly with the oxygen atoms of the α- and γ-phosphate groups and with the bridging N atom. Similarly, the ε-amino group of K68 is rotated by ~180° with respect to its position in chain A and forms an ionic interaction with E154, which in turn forms a salt bridge with R108. Comparison of the structures of MeaB with other G-proteins such as HypB[24], suggest that residues E154 and D105 serve as Mg^{2+} ligands. Thus, E154 is likely to disengage from R108 to bind to Mg^{2+} in the activated MeaB:MCM complex.

The available MeaB structures have fairly similar dimeric arrangements and overall conformations as evidenced by their small comparative rmsd values (Supplementary Table 2). The main differences are evident in the P-loop, switch-I and -II regions, and most significantly, in the switch III region. The switch III loop is found in one of three

conformations or is disordered. We postulate that switch III exists in an ensemble of conformations and that the equilibrium between these conformations is influenced by the nucleotide bound in the active site in the MCM:MeaB complex. The substantial conformational flexibility of the switch III region prompted us to test its potential role in signaling.

Alanine Scanning Mutagenesis of Switch III Loop

The following switch III residues conserved in MeaB-like proteins (Fig. 2) were targeted for substitution with alanine: D182, E183, Q185, and K188. The resulting mutant proteins retained the ability to form high affinity complexes with apo-MCM yielding K_D values ranging from 61 ± 9 to 117 ± 17 nM in the absence and from 30 ± 13 to 65 ±14 nM in the presence of GMPPNP and exhibited similar thermodynamic parameters as wild-type MeaB (Supplementary Table 3). The affinity of the two MeaB active sites for nucleotide is unequal (Supplementary Table 4). The K_Ds for GMPPNP in the mutants were comparable to that of wild-type MeaB indicating that the mutations in switch III do not significantly impact binding of GMPPNP, particularly at site 1. The K_Ds for GDP binding to the mutant MeaBs were also comparable to the wild-type protein within a 2- to 3-fold range (Supplementary Table 4) as were the nucleotide affinities in the MeaB•apo-MCM complex, which were within a 5–8-fold range (Supplementary Table 5). Interestingly, the stoichiometry of nucleotide binding to MeaB changes from two in the absence to one in the presence of MCM indicating half of sites activity of MeaB in the complex. Collectively, these results establish that the switch III mutations do not significantly perturb binding of nucleotides to MeaB or complex formation between MeaB and apo-MCM.

GAP function of MCM is Impaired in Switch III Mutants

The intrinsic GTPase activity of the switch III mutants is low (k_{obs} = 0.039 to 0.043 min^{-1}) and comparable to that of wild-type MeaB (Table 1). The GAP function of MCM elicits a 100-fold enhancement of the GTPase activity in wild-type MeaB, which is suppressed 10- to 25-fold in the mutants with Q185A and K188A showing the largest impairment. The presence of AdoCbl had no effect on the GAP activity of MCM (data not shown). Mg^{2+} is not required for nucleotide binding and in its absence MeaB binds GDP (K_D = 1.4 ± 0.1 μM and 7.9 ± 2.1 μM for sites 1 and 2) and GMPPNP (0.9 ± 0.2 μM and 6.7 ± 1.7 μM for sites 1 and 2) albeit with slightly lower affinity. The K_{act} for Mg^{2+} in the GTPase assay decreases from 225 ± 22 μM in the absence to 27 ± 8 μM in the presence of MCM (Supplementary Figure 3b). The 10-fold decrease in the K_{act} for Mg^{2+} in the presence of MCM is consistent with the organization of a higher affinity binding-site in the complex versus in MeaB alone. We speculate that the occurrence of an incomplete active site in MeaB alone is a strategy for suppressing its intrinsic GTPase activity, which is activated in the MCM:MeaB complex. Collectively, these results indicate that the switch III loop is important for transmitting the GAP function of MCM to MeaB, which is expressed in part by promoting high-affinity binding of Mg^{2+}.

AdoCbl Loading into MCM is Impaired in Switch III Mutants

ATR catalyzes the transfer of the 5′-deoxyadenosyl group of ATP to cob(I)alamin to form the active cofactor, AdoCbl. However, in addition to functioning as an enzyme in the cobalamin assimilation pathway, ATR also functions as an escort, transferring AdoCbl directly to the MCM:MeaB complex in a process that is gated by GTP hydrolysis by MeaB[6,25–27] and driven by binding of ATP to ATR[26] (Fig. 3a). ATP binding triggers the transfer of one of two bound equivalents of AdoCbl from ATR to the wild-type MCM:MeaB complex in the presence of GTP or the release of AdoCbl into solution in the presence of the non-hydrolyzable analog, GMPPNP[26] (Fig. 3b, *inset*).

Mutations in the switch III region corrupt GTPase-gated inter-protein cofactor transfer (Fig. 3b–c). Hence, in the presence of ATP, ~1 equivalent of AdoCbl is transferred from the ATR to the MCM active site in the presence of GMPPNP rather than being released into solution as seen with wild-type MeaB (Fig. 3c). These results suggest that switch III mutations render AdoCbl transfer from ATR to the MCM:MeaB complex, GTP-independent, corrupting a GTPase-dependent gating mechanism used by wild-type MeaB[6].

Switch III Mutants Affect MCM Turnover and Repair

The reaction catalyzed by MCM involves radical intermediates and is prone to inactivation. We have previously shown that loss of the 5′-deoxyadenosine moiety from the active site, which precludes reformation of AdoCbl at the end of the catalytic cycle, is “sensed” by MeaB and triggers cofactor ejection in a process that utilizes the binding energy of GTP[6]. Inactivation of MCM during enzyme-monitored turnover can be followed spectrophotometrically by formation of aquocobalamin (H_2OCbl, 351 nm) (Fig. 3d–e). Under steady-state turnover conditions, H_2OCbl forms at a rate of 9.5×10^{-3} min^{-1} in the MCM:MeaB complex in the absence of nucleotides. The presence of GTP decreases cofactor oxidation ~30-fold ($k_{obs} = 3.0 \times 10^{-4}$ min^{-1}). While the switch III mutant E183A protects MCM from oxidation to a similar degree as wild-type MeaB (data not shown), the K188A ($k_{obs} = 0.9 \times 10^{-4}$ min^{-1}) and Q185A ($k_{obs} = 1.7 \times 10^{-4}$ min^{-1}) mutants offer less protection. In contrast, the protective capacity of the D182A mutant is substantially diminished. The k_{obs} for oxidative inactivation of MCM in the presence of D182A MeaB and GTP, GMPPNP and GDP are 8.9, 8.4 and 8.2×10^{-3} min^{-1}, respectively and corresponds to an ~30-fold increase compared to wild-type MeaB (Fig. 3e).

We have previously demonstrated that in the presence of nucleotides, MeaB facilitates the ejection of cob(II)alamin if 5′-deoxyadenosine is lost from the MCM active site[6]. To assess the role of the switch III loop in rescue of MCM, cob(II)alamin was mixed with an excess of apo-MCM in complex with the MeaB mutants followed by addition of GMPPNP. The amount of free (i.e. released) cob(II)alamin obtained in the filtrate following centrifugation was then estimated. In the presence of D182A, Q185A and K188A, ~50–60% of cob(II)alamin remained bound to MCM while ~30% of the cofactor was associated with MCM in the presence of the E183A MeaB mutant (Fig. 3f). In contrast, ~3% of cob(II)alamin was bound to MCM in the presence of wild-type MeaB. Hence the efficacy of cofactor expulsion is reduced 16–20-fold in three of the switch III mutants and 10-fold in the E183 mutant.

Mutations in Switch III Lead to Methylmalonic Aciduria

Switch III mutations, G274S and K276E in human MMAA have been reported recently in patients with methylmalonic aciduria[7]. The intrinsic GTPase activity and affinity for nucleotides or for MCM are largely unaffected in the corresponding MeaB mutants (G186S and K188E) as also seen with the alanine mutations in the switch III region (Supplementary Tables 3–5). The pleiotropic biochemical penalties associated with the patient mutations mimicked in MeaB are virtually identical to the set of alanine mutants described above and impair bidirectional signaling with MCM. Thus, the two patient mutations: (i) diminish the GAP activity of MCM (Table 1), (ii) uncouple AdoCbl transfer from ATR from the GTPase activity of MeaB in the MCM:MeaB complex (Fig. 3c), and (iii) inhibit release of inactive cofactor from MCM (Fig. 3f). In the presence of GMPPNP and either K188E or G186S MeaB, MCM undergoes oxidative inactivation at rates of 4.1×10^{-4} min^{-1} and 2.5×10^{-4} min^{-1}, respectively. These values compare well to that of wild-type MeaB indicating a comparable level of protection against inactivation of MCM during catalytic turnover. These results establish the biological import of the switch III loop in the function of MeaB and by inference, MMAA.

Discussion

In this study, we demonstrate that mutations of the conserved polar residues in the switch III region in MeaB impact several aspects of bidirectional signaling ranging from uncoupling AdoCbl transfer from GTP hydrolysis, to protection against inactivation of MCM, to rescue of inactivated MCM, to GAP signaling from MCM to MeaB (Figs. 3b–f and Table 1). Importantly, switch III mutations do not substantially impair nucleotide binding or hydrolysis by MeaB alone or the affinity of MeaB for MCM (Supplementary Tables 3–5 and Table 1).

Switch III loops, previously considered to be unique to heterotrimeric G-proteins, are deployed for bidirectional conveyance of signals from cell surface receptors to intracellular effector proteins. The switch III loops in the $G\alpha_S$ and $G\alpha_T$ subunits are important for β-adrenergic receptor-dependent adenylate cyclase activation[28] and rhodopsin-dependent cyclic GMP phosphodiesterase activation via transducin[29], respectively. The crystal structure of $G\alpha_S$ revealed acidic residues in switch III that interact with basic ones in switch II and suggested that coupled dynamical changes in these two loop regions might be important for G-protein activation. Indeed, mutation of a conserved glutamate residue in switch III impairs receptor-mediated $G\alpha_S$ activation and the same residue is mutated in a patient with pseudohypoparathyroidism[30]. Mutation of the corresponding E232 residue in transducin decreases its downstream function, i.e. effector activation[29]. Comparison of the crystal structures of $G\alpha_T$ with various nucleotide ligands reveals a network of primarily ionic interactions between switch II and III that differ in the GDP versus GTP bound states[31]. Exchange of GDP by GTP induces conformational changes in switch II, which are propagated to switch III.

We posit that the switch III loop in MeaB and its orthologs are functionally equivalent to the corresponding element in Gα proteins. The switch III regions in the MeaB orthologs, ArgK and MMAA[32] are disordered in the respective crystal structures (Fig. 4a). Although not as

well characterized, human MMAA like MeaB, also protects MCM against oxidative inactivation during turnover and reactivates it in a GTPase-dependent manner[33]. While further work is needed to understand the relationship between nucleotide identity/occupancy and switch III conformation particularly in the MCM:MeaB complex, the observed disorder indicates conformational plasticity of switch III in MeaB and related proteins. In the MeaB•2GMPPNP monomers, K188 in the switch III loop interacts with the backbone carbonyl of V158 and a carboxylate oxygen of E162 in switch II (Fig. 4b), communications that are either broken or rearranged in the other MeaB structures (Supplementary Figure 4). Moreover, D182 in the conformationally mobile switch III loop in the MeaB structures is excursive and found in multiple and divergent orientations (Fig 4c). We postulate that nucleotide hydrolysis triggers a conformational change in the switch I/II regions that is propagated via switch II to switch III, where it modulates upstream (AdoCbl docking) and downstream (protection and rescue of MCM) functions. The lack of sequence homology between the switch III loops in MeaB and the Gα proteins suggests convergent evolution of a signaling strategy.

Online Methods

Plasmids and construction of site-specific mutants

The plasmids containing the *Methylobacterium extorquens* AM1 MCM and ATR were described previously[6]. A synthetic gene (GenScript Corp.) encoding *M. extorquens* AM1 MeaB with a 5′-Nco1 site and 3′-Xho1 site was generated for optimal codon usage in *E. coli*. The synthetic MeaB gene was restriction digested with Nco1 and Xho1 (New England Biolabs) and sub-cloned into a pET-21d(+) (Novagen). Site-directed mutants were generated using a Quikchange II XL site-directed mutagenesis kit (Agilent) using the following mutagenic primers and the corresponding antisense primers:

D182A: 5′-GCCGGGTGCAGGTGCTGAACTGCAAGGCATCAAAAAAGG-3′

E183A: 5′-GCCGGGTGCAGGTGATGCACTGCAAGGCATCAAAAAAGG-3′

Q185A: 5′-GGGTGCAGGTGATGAACTGGCAGGCATCAAAAAAGG-3′

K188A: 5′-GGTGATGAACTGCAAGGCATCGCAAAAGGTATCCTGGAACTG-3′

K188E: 5′-GATGAACTGCAAGGCATCGAAAAAGGTATCCTGGAACTGG-3′

G186S: 5′-GCAGGTGATGAACTGCAAAGCATCAAAAAAGGTATCCTG-3′

Mutations generated according to the Quickchange protocol were confirmed by nucleotide sequence determination at the DNA Sequencing Core Facility (University of Michigan, Ann Arbor).

Enzyme expression and purification

Recombinant MeaB, MCM, ATR, and malonyl-CoA synthetase were expressed and purified from One Shot® BL21 (DE3) chemically competent *E. coli* (Invitrogen) as described previously[6,34,35]. Following purification, the enzymes were stored at −80 °C in 50 mM Hepes buffer, pH 8.0, 0.3 M KCl, 10 mM $MgCl_2$, 5 % glycerol (Buffer A).

Enzymatic synthesis and purification of methylmalonyl-CoA

Recombinant malonyl-CoA synthetase was employed for synthesis of methylmalonyl-CoA as described previously[34]. The identity and purity of the product was determined by HPLC using a known standard[34].

Thermodynamic characterization of complex formation and nucleotide binding

Isothermal titration calorimetry experiments were performed at 10 °C in Buffer A using a VPITC calorimeter (Microcal, Inc.) equipped with a 1.43 ml cell and a 300 μl injection syringe. Prior to each titration, samples were degassed using a ThermoVac degasser (Microcal, Inc.) at 5 °C for 10 min. Each titration was performed at least in duplicate and the data were analyzed using the MicroCal ORIGIN program. Titrations of MeaB with nucleotides were performed with 10–25 μM MeaB protein with 8 μl additions of 150–375 μM GDP or GMPPNP (Sigma). The binding affinity of MeaB to MCM was determined by titrating 4–8 μM apo-MCM ± GMPPNP (250 μM) with 10 μl additions of 50–100 μM MeaB ± GMPPNP (250 μM) (Sigma). The binding of nucleotides to the MCM:MeaB complex (with wild-type or mutant MeaBs) was performed using 7.5–15 μM MeaB and a 2-fold molar excess of MCM to ensure saturation of the MCM:MeaB complex. The complexes were titrated with 8–10 μl aliquots of GDP or GMPPNP ranging in concentration from 100–250 μM. Single- or two-site binding models selected based on Chi-squared distribution values for each model, were used to estimate the association constant, K_A, entropy, $T\Delta S^o$, and enthalpy, ΔH^o values. The Gibbs free energy, ΔG^o, was calculated using the following equation: $\Delta G^o = \Delta H^o - T\Delta S^o$.

The effect of switch III mutants on oxidative inactivation of MCM

The inactivation of MCM under steady-state turnover conditions in the presence of MeaB ± GMPPNP or GDP was followed by UV/visible spectroscopy by monitoring conversion of MCM-bound AdoCbl to H_2OCbl at 20 °C[12]. To generate the MCM:MeaB complex in 50 mM potassium phosphate, pH 7.5, containing 10 mM $MgCl_2$, 3–4 mM GMPPNP was added to 35–40 μM MeaB and incubated at 20 °C prior to reconstitution with 25–30 μM MCM reconstituted with an equimolar concentration of AdoCbl. An excess of MeaB•2GMPPNP was added to MCM to fully populate the MCM:MeaB complex. The reaction was initiated by addition of methylmalonyl-CoA to a final concentration of 7–10 mM. The rate of inactivation was monitored at 351 nm and plotted as a function of time. The data were fit to a single-exponential equation, $A = A_o - A_p e^{(-kt)}$, where A is the absorbance at 351 nm, A_o represents the initial absorbance of cobalamin, A_p is the final amplitude for the conversion of AdoCbl to H_2OCbl, and k is the rate constant for H_2OCbl formation during turnover. The goodness of fit was evaluated according to the R^2 value using a cutoff R^2 value of 0.95 for each data set. The data shown are representative of at least two independent experiments.

Cofactor transfer assays

The transfer of AdoCbl from holo-ATR to MCM in the MCM:MeaB•GMPPNP complex was performed in the presence of stoichiometric holo-ATR and an excess of GMPPNP, following addition of excess ATP. The transfer or release of AdoCbl was monitored by UV/visible spectroscopy at 20 °C in Buffer A as described previously[6]. Two equivalents of

AdoCbl were added to ATR to generate holo-ATR. The apo-MCM:MeaB•GMPPNP complex was reconstituted by mixing MCM with two equivalents of MeaB and 1 mM GMPPNP in Buffer A. The two enzyme solutions were then mixed to obtain a final concentration of 15 μM holo-ATR (30 μM in bound AdoCbl) and 15 μM of the MCM:MeaB•GMPPNP complex. In control samples, the reaction mixture was centrifuged at this stage using a Centricon YM10 concentrator (4 °C, 30 min., 16,000 × *g*) (Millipore). The presence of the "base-off" absorption spectrum of ATR-bound AdoCbl (λ_{max} = 458 nm) verified that ATR did not release AdoCbl into solution upon sample dilution (i.e. when the MCM:MeaB•GMPPNP solution was added to it). AdoCbl transfer/release was then initiated by addition of 10 mM ATP and the amount of AdoCbl released was calculated using $\Delta\varepsilon_{525}$ = 6.69 mM^{-1} cm^{-1}. The amount of AdoCbl transferred to the MCM active site was independently determined by centrifugation of the mixture through a Centricon YM10 concentrator (4 °C, 30 min., 16,000 × *g*) (Millipore) and determining the concentration of AdoCbl in the filtrate using an ε_{525} = 8.0 mM^{-1} cm^{-1}. The average ± S.D. of ≥3 independent experiments was used for reporting these results.

Cob(II)alamin release assays

Loss of cob(II)alamin from MCM in the presence of MeaB was evaluated under anaerobic conditions in the dark, following taddition of excess GMPPNP. The released cob(II)alamin was quantified by absorption spectroscopy of H_2OCbl (formed upon air oxidation) following separation of bound and free cofactor. Briefly, MCM (25–40 μM) was mixed with a 1.5-fold excess of D182A, E183A, Q185A, G186S, K188E, or K188A MeaB and incubated for 10 min with 20–35 μM cob(II)alamin at 20 °C in anaerobic Buffer A. Then, GMPPNP was added to a final concentration of 1–2 mM and the mixture was incubated for 10 min at 20 °C. The sample was then removed from anaerobic conditions, incubated at 20 °C, and cob(II)alamin was converted to H_2OCbl by air oxidation for 2 h before filtration through a Centricon YM10 concentrator (Millipore). H_2OCbl does not dissociate from the MCM:MeaB•GMPPNP complex[6]. The UV/visible spectra of total and released cofactor were recorded in the unfiltered sample and the filtrate, respectively. The concentration of bound and free cob(II)alamin was determined using ε_{350} = 26.2 $mM^{-1}cm^{-1}$. The percentage of inactive cofactor bound was determined as the average ± S.D. of ≥2 independent experiments.

GTPase activity of MeaB mutants

The k_{cat} values for GTP hydrolysis by wild-type and mutant MeaB in the presence or absence of a 2-fold molar excess of MCM were determined under V_{max} conditions using a discontinuous HPLC assay at a fixed and a saturating concentration of GTP (10 mM) and 10 mM Mg^{2+} at 20 °C in Buffer A. To study the dependence of the GTPase activity on Mg^{2+}, 1 mM GTP and a variable concentration of Mg^{2+} (0–3 mM) was employed in Buffer A at 20 °C. Briefly, reactions were quenched at 10, 20, or 30 min using 10% (vol/vol) 2 N trichloroacetic acid and centrifuged (4 °C, 10 min, 16,000 × *g*) to remove precipitated protein. The samples were then applied to a μ Bondapak HPLC column (Waters) (NH2 10 μm, 125 Å 3.9 × 300 mm) and the eluent was monitored at 254 nm. GTP and GDP were separated using the following HPLC program at a flow rate of 1 ml/min: 100% of Buffer 1 (0.05 M potassium phosphate, pH 4.5) from 0–5 minutes, a linear gradient to 70 % Buffer 2

(0.80 M potassium phosphate, pH 4.5) from 5–20 min, isocratic elution with 70% Buffer 2 from 20–25 min, a linear gradient of 0 to 100% Buffer 1 from 25–26 min and isocratic elution with 100% Buffer 1 from 26–35 min. Under these conditions, GTP and GDP eluted at ~15.5 min and ~11.8 min, respectively. Values of k_{cat} ± S.D. represent the average at least 3 independent experiments.

Crystallization and crystal harvesting

Crystals of apo-MeaB and MeaB•2GMPPNP were obtained at 4 °C and 20 °C, respectively, by the vapor diffusion method from 4 μl 1:1 mixtures of protein to reservoir solutions. All protein samples were concentrated to 11 mg/ml in 50 mM Hepes buffer, pH 8.0, 2.5 mM $MgCl_2$, 5 mM GMPPNP and 5 % glycerol for MeaB with GMPPNP co-crystallization and in 50 mM Hepes buffer, pH 8.0, 2.5 mM $MgCl_2$, and 5 % glycerol for apo-MeaB. The reservoir solutions contained 28 % PEG400 in 50 mM HEPES, pH 7.5, for apo-MeaB, and 28 % PEG550MME in 50 mM MES, pH 6.5 for MeaB with GMPPNP. Crystals of MeaB with GMPPNP were cryoprotected for a few minutes prior to flash freezing in liquid N_2, by transfer to a solution of 22 % glycerol, 5 mM GMPPNP and 21 % PEG550MME in 50 mM MES pH 6.75. Crystals of apo-MeaB were harvested directly from the crystallization drop and were subsequently flash frozen in liquid N_2. Crystals of MeaB with GMPPNP were of space group *C*2 (a= 185.6, b= 58.2, c= 76.4, β= 106.3) with 2 monomers in the asymmetric unit. Crystals of apo-MeaB were of space group *C*2 (a= 185.5, b= 58.4, c= 155.3, β= 110.1) with 4 monomers in asymmetric unit.

Data collection and structure determination

Diffraction data for apo-MeaB and MeaB•2GMPPNP were collected at 100 K on beamline GM/CA-CAT 23-ID-D at the Advanced Photon Source, Argonne National Laboratory (Argonne, IL). Data for apo-MeaB and MeaB•2GMPPNP were recorded on a Mar300 detector and processed with XDS[36] to 2.2 Å, and 2.1 Å resolution respectively. Phases were obtained by molecular replacement with the program PHASER[37] using a single monomer of the MeaB•GDP structure[22] (PDB ID 2QM7) as a search model. Loops containing residues 62-67, 95-100, 181-186, and 225-231 were removed from the search model to eliminate bias. Initial simulated annealing refinement (torsional and cartesian) was performed for the model obtained from molecular replacement with phenix.refine[38] in order to remove potential model bias. Subsequently, restrained individual atomic refinement, and restrained isotropic individual B-factor refinement with maximum likelihood targets using the Babinet model for bulk solvent scaling was performed using REFMAC5[39] of the CCP4 suite[40]. COOT[41] was used to manually correct the incorrectly modeled residues. Through successive iterative rounds of refinement and manual model building, the remaining residues were traced in the electron density to afford the structural models. In later rounds of refinement, electron density near the nucleotide binding sites for one chain in Apo-MeaB and in both chains in MeaB•GMPPNP, were assigned and modeled with GDP and GMPPNP respectively. Crystallographic information as well as refinement statistics are provided in Supplementary Table 1. The geometric quality of the models was assessed with MolProbity[42]. For Apo-MeaB, Molprobity reported a clash and a Molprobity score of 4.5 (99th percentile) and 1.73 (95th percentile) respectively, while 97.2% of the residues were in the favored Ramachandran plot regions with 3 outliers (0.24%). For MeaB•2GMPPNP

Molprobity reported a clash and a molprobity score of 4.59 (99th percentile) and 1.54 (97th percentile) respectively, while 98.1% of the residues were in the favored Ramachandran plot regions with no outliers. PyMOL[43] was used to create molecular images.

Summary of Statistical Analysis

Kinetic data were analyzed using either Kaleidograph or Microsoft Excel. MicroCal Origin was used to determine Chi-squared distribution of one- and two-site models ITC calorimetric titrations.

Accession Codes

The crystal structure coordinates for MeaB•2GMPPNP and Apo-MeaB were deposited to the RCSB Protein Data Bank under PDB codes 4JYB and 4JYC, respectively.

Supplementary Material

Refer to Web version on PubMed Central for supplementary material.

References Listed

1. Boal AK, Rosenzweig AC. Structural biology of copper trafficking. Chem Rev. 2009; 109:4760–4779. [PubMed: 19824702]
2. Gherasim C, Lofgren M, Banerjee R. Navigating the B_{12} road: assimilation, delivery and disorders of cobalamin. J Biol Chem. 2013; 288:13186–13193. [PubMed: 23539619]
3. Reddi AR, Jensen LT, Culotta VC. Manganese homeostasis in *Saccharomyces cerevisiae*. Chem Rev. 2009; 109:4722–4732. [PubMed: 19705825]
4. Korotkova N, Lidstrom ME. MeaB is a component of the methylmalonyl-CoA mutase complex required for protection of the enzyme from inactivation. J Biol Chem. 2004; 279:13652–13658. [PubMed: 14734568]
5. Dobson CM, et al. Identification of the gene responsible for the *cbl*A complementation group of vitamin B_{12}-responsive methylmalonic acidemia based on analysis of prokaryotic gene arrangements. Proc Natl Acad Sci U S A. 2002; 99:15554–15559. [PubMed: 12438653]
6. Padovani D, Banerjee R. A G-protein editor gates coenzyme B_{12} loading and is corrupted in methylmalonic aciduria. Proc Natl Acad Sci U S A. 2009; 106:21567–21572. [PubMed: 19955418]
7. Dempsey-Nunez L, et al. High resolution melting analysis of the MMAA gene in patients with cblA and in those with undiagnosed methylmalonic aciduria. Mol Genet Metab. 2012; 107:363–367. [PubMed: 23026888]
8. Banerjee R. Radical carbon skeleton rearrangements: catalysis by coenzyme B_{12}-dependent mutases. Chem Rev. 2003; 103:2083–2094. [PubMed: 12797824]
9. Ledley FD, Lumetta M, Nguyen PN, Kolhouse JF, Allen RH. Molecular Cloning of L-Methylmalonyl CoA Mutase: Gene Transfer and Analysis of mut Mell Lines. Proc Natl Acad Sci US A. 1988; 85:3518–3521.
10. Leipe DD, Wolf YI, Koonin EV, Aravind L. Classification and evolution of P-loop GTPases and related ATPases. J Mol Biol. 2002; 317:41–72. [PubMed: 11916378]
11. Padovani D, Labunska T, Banerjee R. Energetics of interaction between the G-protein chaperone, MeaB and B_{12}-dependent methylmalonyl-CoA mutase. J Biol Chem. 2006; 281:17838–17844. [PubMed: 16641088]
12. Padovani D, Banerjee R. Assembly and protection of the radical enzyme, methylmalonyl-CoA mutase, by its chaperone. Biochemistry. 2006; 45:9300–9306. [PubMed: 16866376]
13. Hennig SE, Jeoung JH, Goetzl S, Dobbek H. Redox-dependent complex formation by an ATP-dependent activator of the corrinoid/iron-sulfur protein. Proc Natl Acad Sci U S A. 2012; 109:5235–5240. [PubMed: 22431597]

14. Fujii K, Galivan JH, Huennekens FM. Activation of methionine synthase: Further characterization of the flavoprotein system. Arch Biochem Biophys. 1977; 178:662–670. [PubMed: 13738]
15. Olteanu H, Banerjee R. Human methionine synthase reductase, a soluble P-450 reductase-like dual flavoprotein, is sufficient for NADPH-dependent methionine synthase activation. J Biol Chem. 2001; 276:35558–35563. [PubMed: 11466310]
16. Mori K, Tobimatsu T, Hara T, Toraya T. Characterization, sequencing, and expression of the genes encoding a reactivating factor for glycerol-inactivated adenosylcobalamin- dependent diol dehydratase. J Biol Chem. 1997; 272:32034–32041. [PubMed: 9405397]
17. Mori K, Bando R, Hieda N, Toraya T. Identification of a reactivating factor for adenosylcobalamin-dependent ethanolamine ammonia lyase. J Bacteriol. 2004; 186:6845–6854. [PubMed: 15466038]
18. Mori K, Toraya T. Mechanism of reactivation of coenzyme B12-dependent diol dehydratase by a molecular chaperone-like reactivating factor. Biochemistry. 1999; 38:13170–13178. [PubMed: 10529189]
19. Shibata N, et al. Release of a damaged cofactor from a coenzyme B12-dependent enzyme: X-ray structures of diol dehydratase-reactivating factor. Structure. 2005; 13:1745–1754. [PubMed: 16338403]
20. Olteanu H, Banerjee R. Redundancy in the pathway for redox regulation of mammalian methionine synthase: reductive activation by the dual flavoprotein, novel reductase 1. J Biol Chem. 2003; 278:38310–38314. [PubMed: 12871938]
21. Sprang SR, Chen Z, Du X. Structural basis of effector regulation and signal termination in heterotrimeric Galpha proteins. Adv Prot Chem. 2007; 74:1–65.
22. Hubbard PA, et al. Crystal structure and mutagenesis of the metallochaperone MeaB: insight into the causes of methylmalonic aciduria. J Biol Chem. 2007; 282:31308–31316. [PubMed: 17728257]
23. Wittinghofer A, Vetter IR. Structure-function relationships of the G domain, a canonical switch motif. Annu Rev Biochem. 2011; 80:943–971. [PubMed: 21675921]
24. Gasper R, Scrima A, Wittinghofer A. Structural insights into HypB, a GTP-binding protein that regulates metal binding. J Biol Chem. 2006; 281:27492–27502. [PubMed: 16807243]
25. Padovani D, Labunska T, Palfey BA, Ballou DP, Banerjee R. Adenosyltransferase tailors and delivers coenzyme B_{12}. Nat Chem Biol. 2008; 4:194–196. [PubMed: 18264093]
26. Padovani D, Banerjee R. A Rotary Mechanism for Coenzyme B_{12} Synthesis by Adenosyltransferase. Biochemistry. 2009; 48:5350–5357. [PubMed: 19413290]
27. Yamanishi M, Vlasie M, Banerjee R. Adenosyltransferase: an enzyme and an escort for coenzyme B_{12}? Trends Biochem Sci. 2005; 30:304–308. [PubMed: 15950874]
28. Grishina G, Berlot CH. Mutations at the domain interface of GSalpha impair receptor-mediated activation by altering receptor and guanine nucleotide binding. J Biol Chem. 1998; 273:15053–15060. [PubMed: 9614114]
29. Li Q, Cerione RA. Communication between switch II and switch III of the transducin alpha subunit is essential for target activation. J Biol Chem. 1997; 272:21673–21676. [PubMed: 9268292]
30. Ahmed SF, et al. GNAS1 mutational analysis in pseudohypoparathyroidism. Clin Endocrinol. 1998; 49:525–531.
31. Lambright DG, Noel JP, Hamm HE, Sigler PB. Structural determinants for activation of the alpha-subunit of a heterotrimeric G protein. Nature. 1994; 369:621–628. [PubMed: 8208289]
32. Froese DS, et al. Structures of the human GTPase MMAA and vitamin B_{12}-dependent methylmalonyl-CoA mutase and insight into their complex formation. J Biol Chem. 2010; 285:38204–38213. [PubMed: 20876572]
33. Takahashi-Iniguez T, Garcia-Arellano H, Trujillo-Roldan MA, Flores ME. Protection and reactivation of human methylmalonyl-CoA mutase by MMAA protein. Biochem Biophys Res Commun. 2011; 404:443–447. [PubMed: 21138732]
34. Padovani D, Banerjee R. Alternative pathways for radical dissipation in an active site mutant of B_{12}-dependent methylmalonyl-CoA mutase. Biochemistry. 2006; 45:2951–2959. [PubMed: 16503649]

35. Lofgren M, Banerjee R. Loss of allostery and coenzyme B_{12} delivery by a pathogenic mutation in adenosyltransferase. Biochemistry. 2011; 50:5790–5798. [PubMed: 21604717]
36. Otwinowski Z, Minor W. Macromolecular Crystallography, Pt A Vol 276 Methods in Enzymology. 1997:307–326.
37. McCoy AJ, et al. Phaser crystallographic software. Journal of Applied Crystallography. 2007; 40:658–674. [PubMed: 19461840]
38. Adams PD, et al. PHENIX: building new software for automated crystallographic structure determination. Acta Crystallogr D Biol Crystallogr. 2002; 58:1948–1954. [PubMed: 12393927]
39. Murshudov GN, Vagin AA, Dodson EJ. Refinement of macromolecular structures by the maximum-likelihood method. Acta Crystallogr D Biol Crystallogr. 1997; 53:240–255. [PubMed: 15299926]
40. The CCP4 suite: programs for protein crystallography. Acta crystallographica. Section D, Biological crystallography. 1994; 50:760–763. [PubMed: 15299374]
41. Emsley P, Cowtan K. Coot: model-building tools for molecular graphics. Acta Crystallogr D Biol Crystallogr. 2004; 60:2126–2132. [PubMed: 15572765]
42. Davis IW, et al. MolProbity: all-atom contacts and structure validation for proteins and nucleic acids. Nucleic Acids Res. 2007; 35:W375–383. [PubMed: 17452350]
43. Schrodinger LLC. The PyMOL Molecular Graphics System, Version 1.3r1. 2010

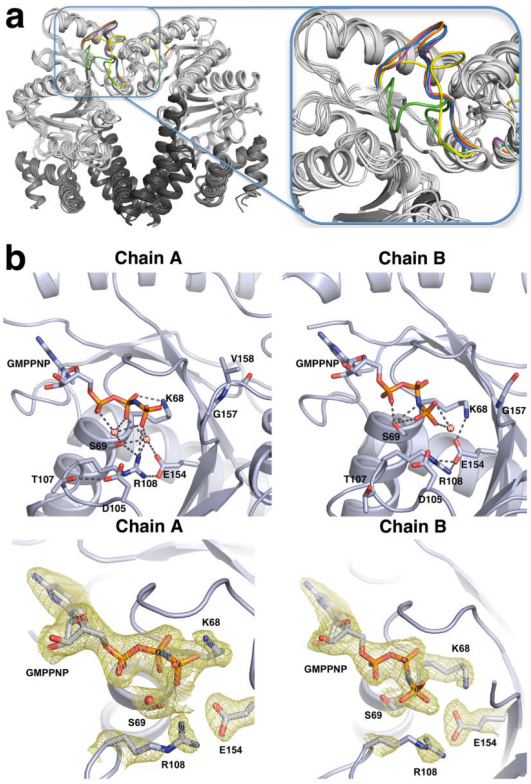

Figure 1. Crystal structure of MeaB reveals a mobile switch III loop

(**a**) Comparison of MeaB crystal structures (gray) and the mobile Switch III regions (various colors). Apo-MeaB (green), MeaB•2GMPPNP (blue), MeaB•2GDP (yellow), MeaB•1GDP (mangenta), MeaB•2Pi (orange). (**b**) Close-up of the two active sites (designated as chains A and B) in the MeaB•2GMPPNP structure showing interactions between active site residues and the nucleotide (top) and composite omit electron density of the two GMPPNP ligands in the active site contoured at 1σ (bottom). The GMPPNP ligands as well as active site residues K68, S69, R108 and E154 are shown in sticks.

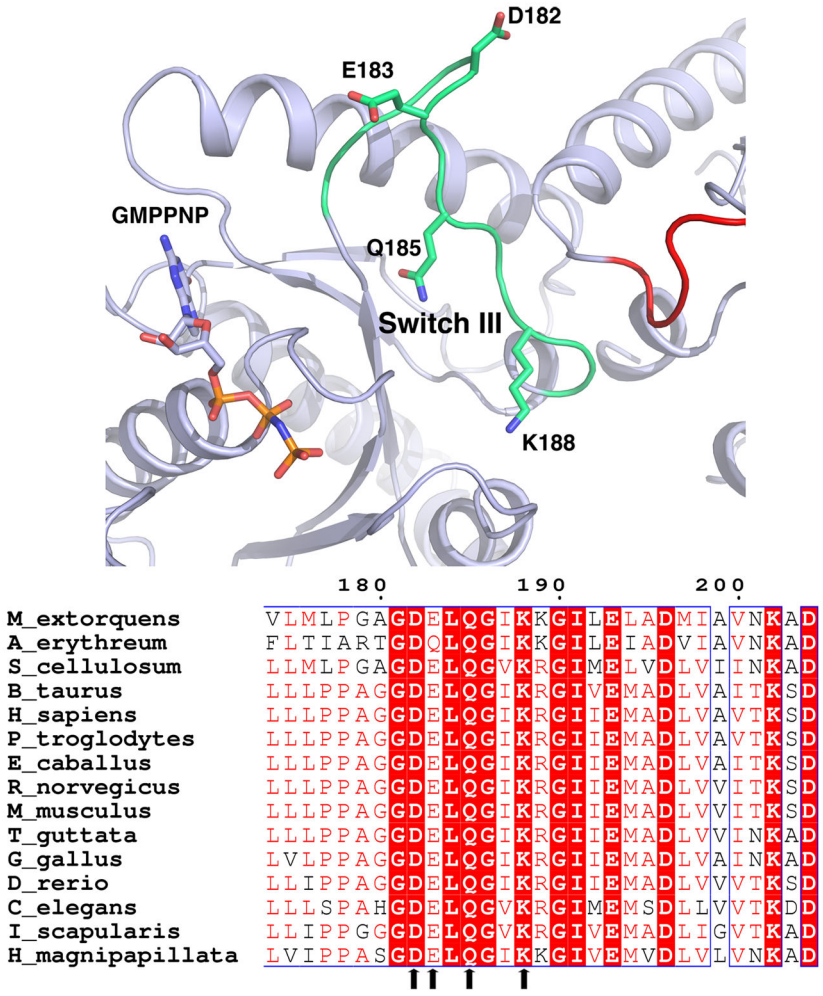

Figure 2. Conservation of Switch III loop residues

Conformation of a switch III loop in the MeaB:2GMPPNP structure (top) and sequence alignment of the switch III sequences of MeaB and its orthologs (bottom). Invariant residues investigated in this study are highlighted with red arrows and mapped in the structure with sticks.

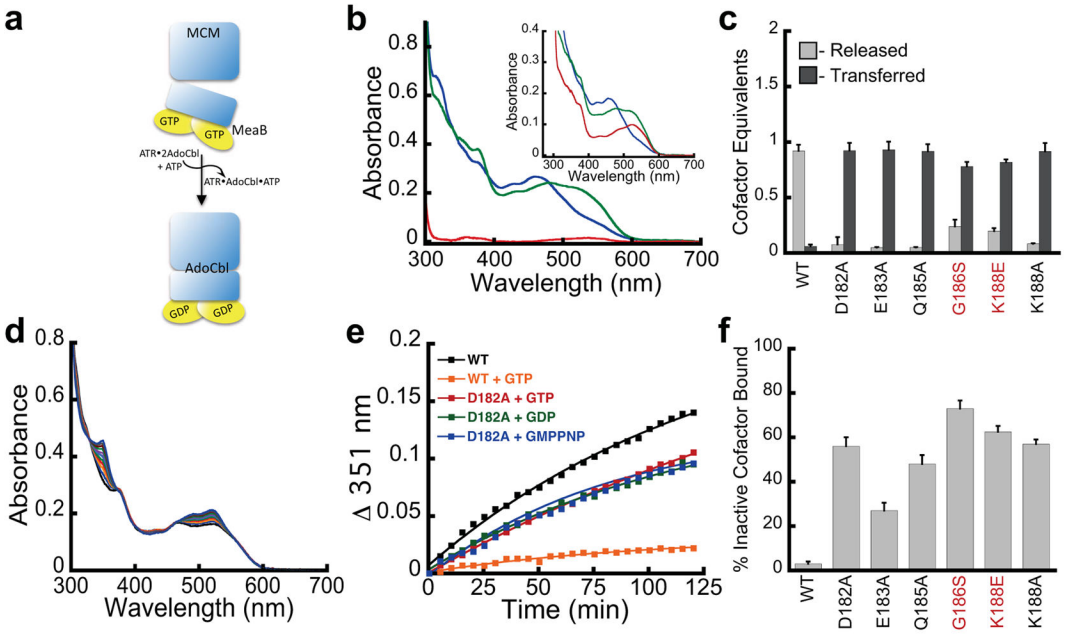

Figure 3. The pleiotropic effects of switch III mutations

(**a**) Model for AdoCbl transfer from ATR to MCM:MeaB gated by GTP hydrolysis and triggered by ATP binding to ATR. (**b**) Representative spectra showing changes associated with the transfer of one of two equivalents of AdoCbl from ATR (blue) to MCM in the MCM:mutant MeaB•2GMPPNP complex (green) upon addition of ATP. Very little cofactor is released into solution (red). The *inset* shows the corresponding spectra in the presence of wild-type MeaB and GMPPNP in which one equivalent of AdoCbl is lost from ATR (blue) to solution (green) following addition of ATP. The red spectrum represents free AdoCbl recovered after filtration. (**c**) Comparison of AdoCbl equivalents transferred to MCM versus released into solution from ATR in the presence of different MeaBs containing bound GMPPNP. (**d**) Spectroscopic changes accompanying oxidative inactivation of MCM during turnover under aerobic conditions. The increase in absorbance at 351 nm corresponds to oxidation of the cob(II)alamin formed during catalytic turnover of MCM, to H_2OCbl. (e) Comparison of the inactivation rates for MCM in the presence of wild-type versus the D182A MeaB with GTP, GMPPNP or GDP. Inactivation was monitored at 351 nm. (**f**) Comparison of inactive cobalamin that remains bound to MCM in the presence of wild-type versus mutant MeaBs with bound GMPPNP. The patient mutations are shown in red in c and f and the data represent the mean ± SD of ≥3 (c) and ≥2 (f) independent experiments as described under Online Methods.

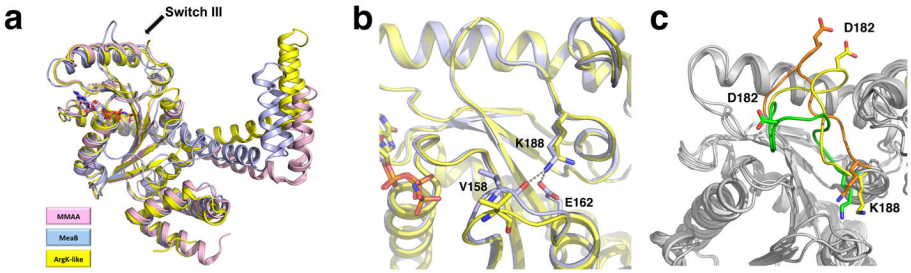

Figure 4. Switch III loop conformations

(a) Superposition of monomers of MeaB•GMPPNP, ArgK-like protein (PDB ID; 2P67) and MMAA (PDB ID; 2WWW). (b) Interactions between the switch III residue, K188 and switch II residues, V158 and E162 in the structures of MeaB•2GDP (yellow) and MeaB•2GMPPNP (blue). (**c**) Position of D182 and K188 in apo-MeaB (green), MeaB•2GDP (yellow), and MeaB•2Pi (orange).

Table 1

Kinetic Parameters for GTP hydrolysis by switch III mutants of MeaB[1].

	k_{cat} (min^{-1})	
Enzyme	**− MCM**	**+ MCM**
Wild-type	0.039 ± 0.003	4.20 ± 0.21
D182A	0.042 ± 0.004	0.50 ± 0.05
E183A	0.040 ± 0.005	0.30 ± 0.04
Q185A	0.043 ± 0.004	0.17 ± 0.03
K188A	0.039 ± 0.001	0.14 ± 0.02
G186S	0.050 ± 0.006	0.21 ± 0.03
K188E	0.047 ± 0.004	0.28 ± 0.02

[1]These experiments were performed as described under online Methods and represent the mean of at least three experiments ± S.D.